Basic Research in Cardiology (2019) 114:13
https://doi.org/10.1007/s00395-019-0720-7

ORIGINAL CONTRIBUTION

Protein kinase/phosphatase balance mediates the effects of increased late sodium current on ventricular calcium cycling

Jörg Eiringhaus[1,2,9] · Jonas Herting[1,9] · Felix Schatter[1,9] · Viacheslav O. Nikolaev[3] · Julia Sprenger[1] · Yansong Wang[4] · Maja Köhn[4,5] · Markus Zabel[1,9] · Ali El-Armouche[6] · Gerd Hasenfuss[1,9] · Samuel Sossalla[1,7,9] · Thomas H. Fischer[1,8,9]

Received: 4 May 2018 / Accepted: 12 February 2019 / Published online: 20 February 2019

Abstract

Increased late sodium current (late I_{Na}) is an important arrhythmogenic trigger in cardiac disease. It prolongs cardiac action potential and leads to an increased SR Ca^{2+} leak. This study investigates the contribution of Ca^{2+}/Calmodulin-dependent kinase II (CaMKII), protein kinase A (PKA) and conversely acting protein phosphatases 1 and 2A (PP1, PP2A) to this subcellular crosstalk. Augmentation of late I_{Na} (ATX-II) in murine cardiomyocytes led to an increase of diastolic Ca^{2+} spark frequency and amplitudes of Ca^{2+} transients but did not affect SR Ca^{2+} load. Interestingly, inhibition of both, CaMKII and PKA, attenuated the late I_{Na}-dependent induction of the SR Ca^{2+} leak. PKA inhibition additionally reduced the amplitudes of systolic Ca^{2+} transients. FRET-measurements revealed increased levels of cAMP upon late I_{Na} augmentation, which could be prevented by simultaneous inhibition of Na^+/Ca^{2+}-exchanger (NCX) suggesting that PKA is activated by Ca^{2+}-dependent cAMP-production. Whereas inhibition of PP2A showed no effect on late I_{Na}-dependent alterations of Ca^{2+} cycling, additional inhibition of PP1 further increased the SR Ca^{2+} leak. In line with this, selective activation of PP1 yielded a strong reduction of the late I_{Na}-induced SR Ca^{2+} leak and did not affect systolic Ca^{2+} release. This study indicates that phosphatase/kinase-balance is perturbed upon increased Na^+ influx leading to disruption of ventricular Ca^{2+} cycling via CaMKII- and PKA-dependent pathways. Importantly, an activation of PP1 at RyR2 may represent a promising new toehold to counteract pathologically increased kinase activity.

Keywords Late sodium current · SR calcium leak · Calcium cycling · CaMKII · PKA · PP1 · PP2A

Introduction

The late Na current (late I_{Na}) is a persisting, low-amplitude Na influx following the initial, fast-inactivating component (peak I_{Na}) in cardiomyocytes [2]. While its physiological role is rather minor, its persistence over hundreds of milliseconds

Jörg Eiringhaus and Jonas Herting contributed equally to this work.

✉ Thomas H. Fischer
thomas.fischer@med.uni-goettingen.de

1 Abt. Kardiologie und Pneumologie/Herzzentrum, Georg-August-Universität Göttingen, Robert-Koch-Str. 40, 37075 Göttingen, Germany

2 Abt. Kardiologie und Angiologie, Medizinische Hochschule Hannover, Hannover, Germany

3 Institut für Experimentelle Herz-Kreislaufforschung, Universitätsklinikum Hamburg-Eppendorf, Hamburg, Germany

4 European Molecular Biology Laboratory, Genome Biology Unit, Heidelberg, Germany

5 Centre for Biological Signalling Studies (BIOSS) and Faculty of Biology, University of Freiburg, Freiburg, Germany

6 Institut für Pharmakologie und Toxikologie, Technische Universität Dresden, Dresden, Germany

7 Klinik und Poliklinik für Innere Medizin II, Universitätsklinikum Regensburg, Regensburg, Germany

8 Medizinische Klinik II, Kardiologie, Angiologie, Pneumologie, Klinikum Coburg, Coburg, Germany

9 Deutsches Zentrum für Herz-Kreislauf Forschung (DZHK), Standort Göttingen, Göttingen, Germany

[24] can lead to a late I_{Na} dependent Na^+ influx even exceeding that of peak I_{Na} once its amplitude is increased under pathological conditions and hereby facilitate intracellular Na^+ overload [5]. Furthermore, the sustained depolarizing inward Na^+ current offsets repolarizing K^+ currents leading to a prolongation of action potential duration (APD) and increased susceptibility to early afterdepolarizations (EADs)[2]. An elevated late I_{Na} was found in several cardiac pathologies such as hypoxia [22], ischemia [23, 31], oxidative stress [39], inflammation [38], channelopathies [30], atrial fibrillation [34] and heart failure [26]. Importantly, late I_{Na} is closely linked to another important pathomechanism in cardiac disease, the disturbance of myocardial Ca^{2+} cycling. Of note, the extrusion of intracellular Na^+ via reverse mode of the sarcolemmal Na^+/Ca^{2+} exchanger (NCX) leads to an increase of intracellular Ca^{2+} concentrations. Our group demonstrated that an elevation of late I_{Na} in ventricular cardiomyocytes increases the instability of diastolic RyR2 closure in the sarcoplasmic reticulum (diastolic SR Ca^{2+} leak) through an activation of Ca^{2+}/Calmodulin dependent kinase II (CaMKII) and subsequently triggers proarrhythmogenic events [32, 37] as an extrusion of Ca^{2+} via NCX can induce delayed afterdepolarization (DADs) through a net influx of positive charge carriers (transient inward current, I_{ti}) [33]. We recently confirmed this pathway in atrial myocardium and additionally found evidence for a late I_{Na}-induced, Ca^{2+}-dependent activation of intracellular adenylylcyclases (ACs) leading to an increased activity of protein kinase A (PKA) [17]. This study, therefore, aims at more comprehensively investigating the functional effects of an increased late I_{Na} on ventricular calcium-cycling and at elucidating the role of both, PKA and CaMKII, in this subcellular crosstalk. Furthermore, this is the first study to evaluate the functional role of conversely acting protein phosphatases (PP) 1 and 2A in this context.

Methods

Myocyte isolation

Isolation of ventricular cardiomyocytes from wild-type (WT) mice (B6N) was performed as reported previously [37]. A Langendorff apparatus was used to retrogradely perfuse the explanted hearts with an initially Ca^{2+} free Tyrode's solution containing (in mmol/L): NaCl 113, KCl 4.7, KH_2PO_4 0.6, $Na_2HPO_4 \times 2H_2O$ 0.6, $MgSO_4 \times 7H_2O$ 1.2, $NaHCO_3$ 12, $KHCO_3$ 10, HEPES 10, Taurine 30, BDM 10, glucose 5.5, phenol-red 0.03 (37 °C, pH 7.4). Afterwards, 7.5 mg/ml liberase 1 (Roche diagnostics, Mannheim, Germany) and trypsin 0.6% (Life Technologies, Carlsbad, CA, USA) as well as 0.125 mmol/L $CaCl_2$ were added to the perfusion solution. Once the tissue had become flaccid, ventricular and atrial myocardium was separated by cutting off the ventricles beneath the atrioventricular valve level. The ventricular myocardium was cut into small pieces and dispersed in Tyrode's solution. The concentration of Ca^{2+} was stepwise increased every 3 min until the target concentration was reached. Cells were plated on laminin-coated recording chambers and left for 20 min to enable settling. To ensure the validity of functional measurements, the structural integrity of investigated cardiomyocytes was an important requirement. Thus, only cell suspensions that contained an adequate fraction of elongated, not granulated cardiomyocytes with cross-striations were selected for experiments.

Selective activation of PP1 in murine myocardium

To evaluate the effects of specific PP1 activation on Ca^{2+} cycling properties in cardiomyocytes, we used PP1-disrupting peptide 3 (PDP3) [9] as previously described [16]. In general, PP1 activity is regulated via the interaction between the catalytic subunit and various regulatory proteins (PP1-interacting proteins, PIPs) and can be modulated by influencing the PP1–PIP interaction [10]. PDP3 was shown to be a proteolytically stable and cell-permeable peptide that specifically disrupts PP1–PIP interactions and thereby increases PP1 activity in living cells without affecting the closely related phosphatase PP2A [9]. We used the inactive variant PDP3m (RATA-mutated) as a control to investigate changes in Ca^{2+} cycling properties upon specific PP1 activation.

Intracellular Ca^{2+} imaging

Confocal microscopy

Titrated concentrations of Anemonia sulcata toxin II (ATX-II, Alomone labs, Jerusalem, Israel, 0.5–5 nmol/L, dependent on the activity of LOT) were used to increase late I_{Na} current in wild-type murine cardiomyocytes to levels found in cardiac disease [21, 25]. ATX-II potently modulates voltage-gated Na^+ channel gating kinetics by delaying its inactivation and subsequently prolongs action potential duration. Isolated cells were incubated at room temperature for 15 min with a Fluo-4-AM loading buffer (Fig. 1) or Fluo-3-AM loading buffer (Figs. 4 and 6, 10 µmol/L each, Molecular Probes, Eugene, OR, USA) which contained: no active agent (control group), ATX-II alone, ATX-II in combination with CaMKII inhibitor Autocamtide-2-related Inhibitory Peptide (AIP, 1 µmol/L, Alexis Corp., Switzerland), ATX-II in combination with PKA inhibitor H89 (5 µmol/L, Sigma–Aldrich, St. Louis, MO, USA), ATX-II in combination with phosphatase inhibitor okadaic acid (OA, 10/100 nmol/L, Enzo Life Sciences, Farmingdale, NY, USA), ATX-II in combination with phosphatase 1 activator phosphatase-1-disrupting-peptide 3 (PDP3, 1 µmol/L, SiChem, Bremen, Germany)

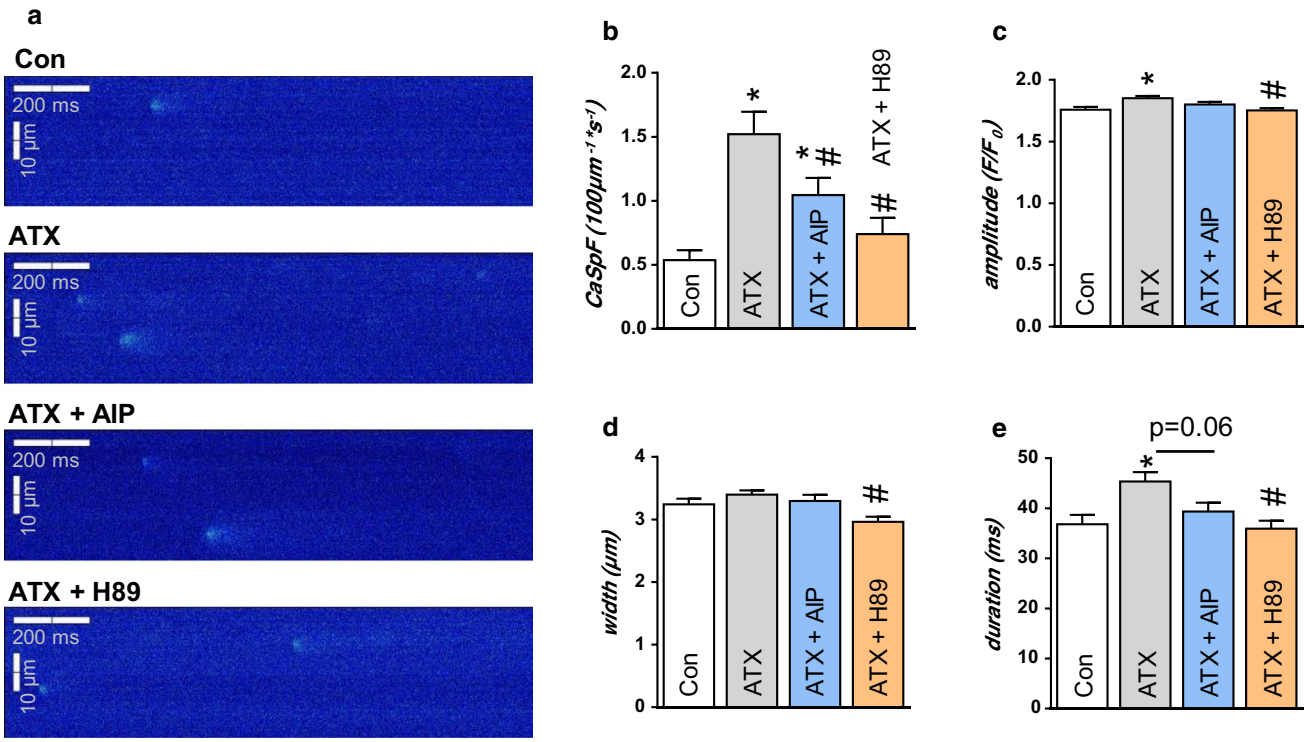

Fig. 1 Effects of late I_{Na} augmentation and modulation of protein kinase activity on diastolic SR Ca^{2+} leak. **a** Representative confocal line scans of murine ventricular cardiomyocytes and respective quantification of **b** CaSpF, as well as **c** amplitude, **d** width and **e** duration of detected Ca^{2+}-sparks. $N = 10$, n (cells/sparks) = 133/185 vs. 118/459 vs. 95/254 vs. 114/224. *significant vs. control; #significant vs. ATX ($P < 0.05$). Drug concentrations: ATX-II 0.5 nmol/L; AIP 1 µmol/L; H89 5 µmol/L

or ATX-II in combination with the inactive form PDP3 m (1 µmol/L, SiChem). AIP was applied in its myristoylated form to ensure cell permeability. OA was used in concentrations of 10 nmol/L to inhibit PP2A and 100 nmol/L to inhibit PP1 and 2A [11].

Experimental solution contained (mmol/L): KCl 4, NaCl 140, $MgCl_2$ 1, HEPES 5, glucose 10, $CaCl_2$ 2 (pH 7.4, NaOH, room temperature) and the respective active agents. To wash out the loading buffer and to remove any extracellular dye, as well as to allow enough time for complete deesterification of the fluorescent dye, cells were incubated with an experimental solution for 15 min before experiments were started. Cells were continuously superfused during experiments. Ca^{2+} spark measurements were performed with a laser scanning confocal microscope (LSM 5 Pascal, Zeiss, Jena, Germany) using a 40× oil-immersion objective. Fluo-3/4-AM was excited by an argon ion laser (488 nm) and emitted fluorescence was collected through a 505 nm long-pass emission filter. Fluorescence images were recorded in the line-scan mode with 512 pixels per line (width of each scanline: 38.4 µm) and a pixel time of 0.64 µs. One image consists of 10,000 unidirectional line scans, equating to a measurement period of 7.68 s. Experiments were conducted at resting conditions after loading the SR with Ca^{2+} by repetitive field stimulation (30 beats at 3 Hz, 20 V). Ca^{2+} spark frequency and dimensions were analyzed with the program SparkMaster for ImageJ [29]. The mean spark frequency of the respective cell (CaSpF) was calculated from the number of sparks normalized to cell width and scan rate (100 μm^{-1} s^{-1}).

Epifluorescence microscopy

Cardiomyocytes were isolated and plated as described above and incubated with a Fura-2–AM loading buffer (10 µmol/L, Molecular Probes) for 15 min. In the intervention groups, the loading buffer also contained the respective active agents as described above for confocal microscopy measurements. After staining, cardiomyocytes were incubated with the respective experimental solution (as described in confocal microscopy) for 15 min before measurements were started to enable complete deesterification of intracellular Fura-2-AM and allow cellular rebalance of Ca^{2+} cycling properties. During measurements, cardiomyocytes were continuously superfused with an experimental solution. Measurements were performed with a Motic AE32 microscope (Speed Fair Co. Ltd, Hong Kong) provided with a fluorescence detection system (ION

OPTIX Corp., Milton MA). Cells were excited at 340 and 380 nm and the emitted fluorescence was collected at 510 nm. Intracellular Ca^{2+} levels were measured as the ratio of fluorescence at 340 and 380 nm (F_{340}/F_{380} nm in ratio units, r.u.). Systolic Ca^{2+} transients were recorded at steady state conditions under constant field stimulation (1 Hz). To assess the SR Ca^{2+} content, we measured the amplitude of caffeine-induced Ca^{2+} transients. After stopping the stimulation during steady-state conditions at 1 Hz, caffeine (10 mmol/L, Sigma–Aldrich) was applied directly onto the cell of interest leading to immediate and complete SR Ca^{2+} release. The recorded Ca^{2+} transients were analyzed with the software IONWizard^{R} (ION OPTIX Corp.).

FRET-measurements and data analysis

Freshly isolated adult mouse ventricular cardiomyocytes from Epac1-camps mice [8] were plated onto laminin-coated cover slides and allowed to settle for 30 min. Afterwards, cover slides carrying isolated cardiomyocytes were mounted in an imaging chamber (Attofluor cell chamber, Invitrogen, Carlsbad, CA, USA) equipped with an electrode. After washing the cells with Tyrode's solution (in mmol/L: KCl 1, NaCl 149, $MgCl_2$ 1, HEPES 5, Glucose 10, $CaCl_2$ 1, pH = 7.54), 400 µl Tyrode's solution were added to the chamber and cardiomyocytes were field stimulated at 1 Hz. FRET-measurements (Förster resonance energy transfer) were performed using an inverted fluorescent microscope (Nikon Ti, Nikon Instruments, Tokyo, Japan) and Micro-Manager software [12]. The FRET donor CFP was excited at 440 nm using a CoolLED light source (CoolLED Ltd., Andover, England). Images were acquired every 10 s in CFP and YFP emission channels with an exposure time of usually 10 ms as described [36]. Cardiomyocytes were incubated in Tyrode's solution with or without the reverse-mode NCX inhibitor KB-R7943 (0.1 mmol/L) [1] for 7 min before start of measurements. After establishing a stable baseline signal, ATX-II (0.5 nmol/L) was added to the imaging chamber. When the ATX-II reaction reached a stable plateau (on average after 5 min) 100 nmol/L isoprenaline (Iso) were added. Cardiomyocytes in the control group were incubated in pure Tyrode's solution for 5 min before Iso was added, to exclude possible time-dependent changes in FRET ratio. Data analysis was performed using Origin 8.5 software (OriginLab Corp., Northhampton, MA, USA) as previously described [7, 36]. To calculate the actual FRET ratio, we corrected for the bleedthrough of the donor fluorescence (CFP) into the acceptor (YFP) channel using the equation: FRET Ratio = (YFP − 0.63 × CFP)/CFP. For statistical comparison and graphical representation, the FRET ratio of each experiment was normalized to the baseline signal of the respective cell.

Statistics

All data are presented as mean ± SEM. ANOVA with Holm-Šídák post hoc test was used for statistical analysis. Values of $P < 0.05$ were considered as statistically significant.

Results

Effects of late I_{Na} augmentation and modulation of protein kinase activity on SR Ca^{2+} leak

The impact of selective late I_{Na} augmentation on SR Ca^{2+} leak was investigated by confocal microscopy (Fluo-4-AM). ATX-II was used for augmentation of late I_{Na} as described before [17, 32]. CaMKII (AIP, 1 µmol/L) or PKA (H89, 5 µmol/L) were additionally inhibited in the respective groups to elucidate interconnecting pathways.

An augmentation of late I_{Na} led to a significant increase of Ca^{2+}-spark frequency (CaSpF) of murine ventricular cardiomyocytes by 183 ± 34% in comparison to control conditions (CaSpF ATX-II vs. control = 1.52 ± 0.18 vs. 0.54 ± 0.08 × 100 μm^{-1} s^{-1}, $P < 0.01$, Fig. 1b). Furthermore, ATX-II significantly raised the amplitude (F/F_0: 1.85 ± 0.02 vs. 1.76 ± 0.02, $P < 0.01$, Fig. 1c), and duration (45.35 ± 1.87 vs. 36.83 ± 1.86 ms, $P < 0.01$, Fig. 1e) of detected Ca^{2+}-sparks, with no major effect on Ca^{2+}-spark width (3.40 ± 0.07 vs. 3.24 ± 0.09 µm, $P = 0.50$, Fig. 1d). Simultaneous CaMKII-inhibition led to a pronounced attenuation of the ATX-II dependent induction of CaSpF (ATX-II + AIP vs. ATX-II = 1.05 ± 0.13 vs. 1.52 ± 0.18 × 100 μm^{-1} s^{-1}, $P < 0.05$, Fig. 1b). Ca^{2+}-spark amplitude (F/F_0: 1.80 ± 0.02 vs. 1.85 ± 0.02, $P = 0.15$, Fig. 1c), Ca^{2+}-spark width (3.30 ± 0.10 vs. 3.40 ± 0.07 µm, $P = 0.60$, Fig. 1d) and Ca^{2+}-spark duration were not significantly affected by CaMKII-inhibition (39.35 ± 1.79 vs. 45.35 ± 1.87 ms, $P = 0.06$, Fig. 1e). Slightly different effects were detected when PKA was inhibited: Here, we also found a significant reduction of CaSpF (ATX-II + H89 vs. ATX-II = 0.74 ± 0.13 vs. 1.52 ± 0.18 × 100 μm^{-1} s^{-1}, $P < 0.01$, Fig. 1b). In contrast to CaMKII-inhibition, however, Ca^{2+}-spark amplitude (F/F_0: 1.75 ± 0.02 vs. 1.85 ± 0.02, $P < 0.01$, Fig. 1c), width (2.96 ± 0.08 vs. 3.40 ± 0.07, $P < 0.001$, Fig. 1d) and duration (35.94 ± 1.59 vs. 45.35 ± 1.87 ms, $P < 0.01$, Fig. 1e) were additionally reduced upon PKA inhibition vs. sole ATX-II treatment.

Effects of late I_{Na} augmentation and modulation of protein kinase activity on systolic Ca^{2+} release and SR Ca^{2+} load

The influence of late I_{Na} augmentation on ventricular Ca^{2+} cycling properties was analyzed by epifluorescence

microscopy (Fura-2-AM). Cardiomyocytes were stimulated at 1 Hz to record systolic Ca^{2+} transients and caffeine was applied to quantify SR Ca^{2+} content (Fig. 2a). An augmentation of late I_{Na} did not significantly affect systolic Ca^{2+} transient amplitude (F_{340}/F_{380}: ATX-II vs. control = 0.34 ± 0.02 vs. 0.29 ± 0.01, $P = 0.10$, Fig. 2b) and decay kinetics of systolic Ca^{2+} transients (RT_{80}: 0.29 ± 0.01 vs. 0.32 ± 0.01 s, $P = 0.08$, Fig. 2c) compared to control. Surprisingly, late I_{Na} induction did also not influence the amplitude of caffeine-induced Ca^{2+} transients (F_{340}/F_{380}: 0.49 ± 0.04 vs. 0.54 ± 0.03, $P = 0.46$, Fig. 2d) suggesting unaltered SR Ca^{2+} content despite an increased diastolic SR Ca^{2+} leak (see Fig. 1).

Of note, CaMKII-inhibition did not change late I_{Na}-mediated effects on systolic Ca^{2+} release and diastolic Ca^{2+} elimination. The amplitude (F_{340}/F_{380}: ATX-II + AIP vs.

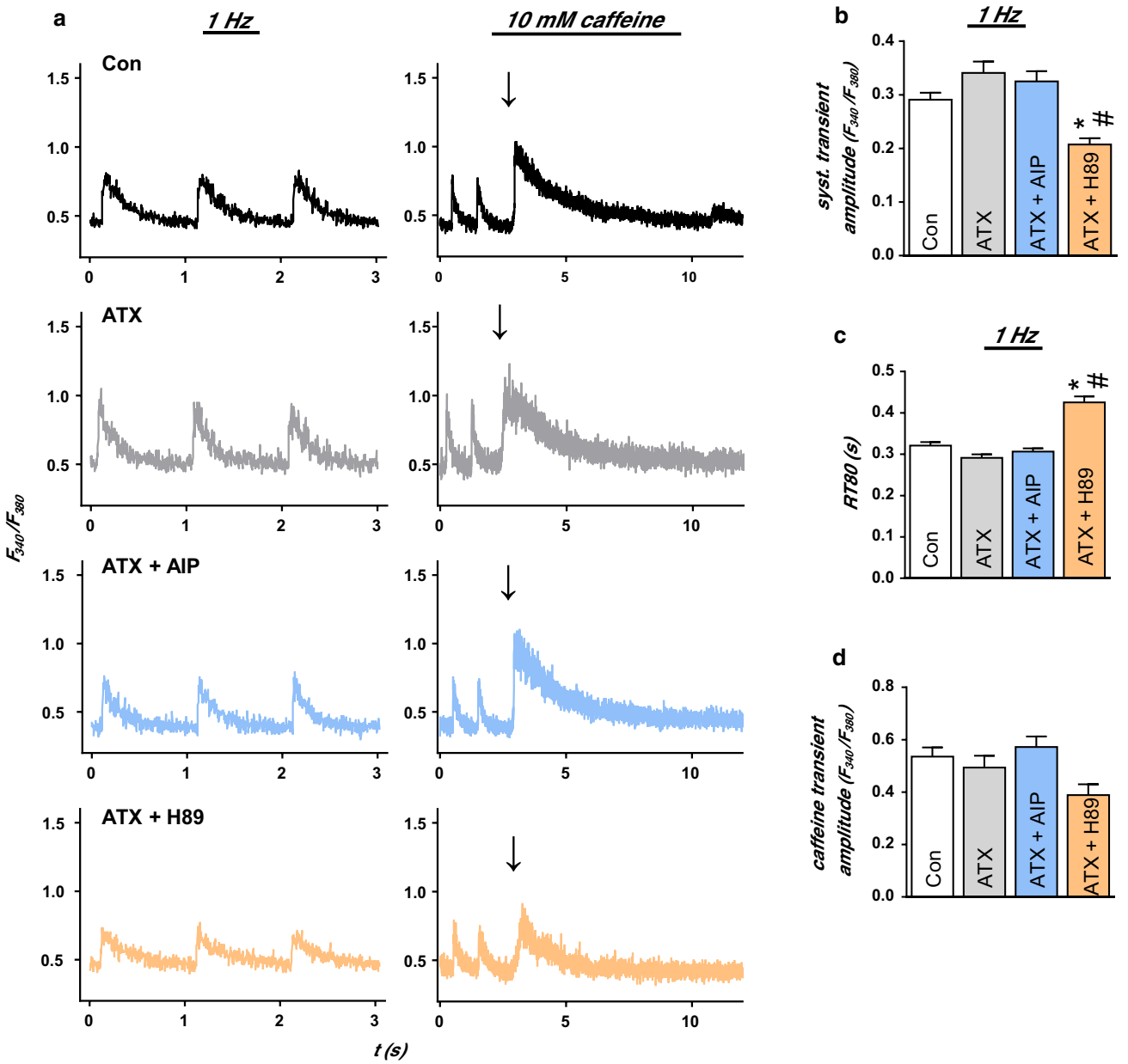

Fig. 2 Effects of late I_{Na} augmentation and modulation of protein kinase activity on Ca^{2+} cycling properties of murine ventricular cardiomyocytes (epifluorescence, Fura-2-AM). **a** Representative original recordings of systolic (1 Hz, left) and caffeine-induced Ca^{2+} transients (right, arrow indicates caffeine application) and respective quantification of **b** systolic Ca^{2+} transient amplitude and **c** decay kinetics (RT_{80}) ($N = 9$, n (cells) = 66 vs. 51 vs. 64 vs. 49), as well as **d** amplitude (peak h) of caffeine-induced Ca^{2+}-transients ($N = 9$; n (cells) = 22 vs. 16 vs. 22 vs. 17). *significant vs. control; #significant vs. ATX ($P < 0.05$). Drug concentrations: ATX-II 0.5 nmol/L; AIP 1 µmol/L; H89 5 µmol/L

ATX-II = 0.34 ± 0.02 vs. 0.33 ± 0.02, $P = 0.51$, Fig. 2b) and decay kinetics of systolic Ca^{2+}-transients (RT_{80}: 0.31 ± 0.01 vs. 0.29 ± 0.01, $P = 0.45$, Fig. 2c), as well as SR Ca^{2+} content (F_{340}/F_{380}: 0.57 ± 0.04 vs. 0.49 ± 0.04, $P = 0.44$, Fig. 2d) did not significantly differ from sole ATX-II treatment. In contrast, inhibition of PKA lowered the amplitude of systolic Ca^{2+}-transients in comparison to sole ATX-II treatment and even below the control values (ATX-II + H89 vs. ATX-II vs. control = F_{340}/F_{380}: 0.21 ± 0.01 vs. 0.34 ± 0.02 vs. 0.29 ± ,0.01, $P < 0.01$, respectively, Fig. 2b). Furthermore, inhibition of PKA significantly slowed Ca^{2+} elimination kinetics compared to sole ATX-II treatment as well as compared to untreated control (RT80: ATX-II + H89 vs. ATX-II vs. control = 0.42 ± 0.01 vs. 0.29 ± 0.01 vs. 0.32 ± 0.01 s; $P < 0.001$, respectively, Fig. 2c). The effect on the amplitude of caffeine-induced transients was not significant (F_{340}/F_{380}: ATX-II + H89 vs. ATX-II = 0.39 ± 0.04 vs. 0.49 ± 0.04, $P = 0.31$, Fig. 2d).

Effects of late I_{Na} augmentation on intracellular cAMP levels

The results described above indicate that an elevated late I_{Na} leads to increased PKA activation, which partly accounts for its effects on Ca^{2+} cycling. To further elucidate the mechanism underlying PKA activation, we determined cytoplasmic cAMP levels in ventricular cardiomyocytes of EPAC-camps transgenic mice using FRET measurements. These mice express a genetically engineered protein (EPAC-camps) that harbours two fluorophores (GFP, YFP). Upon cAMP binding, the distance between both fluorophores increases and resonance energy transfer is reduced providing the possibility of real-time measurements of cytoplasmic cAMP levels in living cells (also see "Methods").

Indeed, cAMP levels rose upon late I_{Na} augmentation by ATX-II compared to time-matched control (YFP/CFP ratio: 0.95 ± 0.01 vs. 0.99 ± 0.00, $P < 0.001$, Fig. 3a, b and d. This response made up for 33% of the maximal isoproterenol (Iso; 100 nmol/L) response. As a Ca^{2+}-dependent mechanism could be assumed, an inhibitor of NCX reverse mode (KB-R7943) was applied to prevent Na^+-induced Ca^{2+} overload [1]. Interestingly, pre-treatment with KB-R7943 significantly diminished the ATX-II effect on cytoplasmic cAMP levels (YFP/CFP ratio: 0.98 ± 0.00 vs. 0.95 ± 0.01, $P < 0.001$, Fig. 3c, d).

Effects of PP1 and PP2A inhibition on late I_{Na} dependent induction of the SR Ca^{2+} leak

The impact of phosphatase inhibition on diastolic SR Ca^{2+} leak in the setting of an elevated late I_{Na} was investigated by confocal microscopy scans (Fluo-3-AM). PP2A (10 nmol/L OA) or PP1 and PP2A (100 nmol/L OA) were inhibited

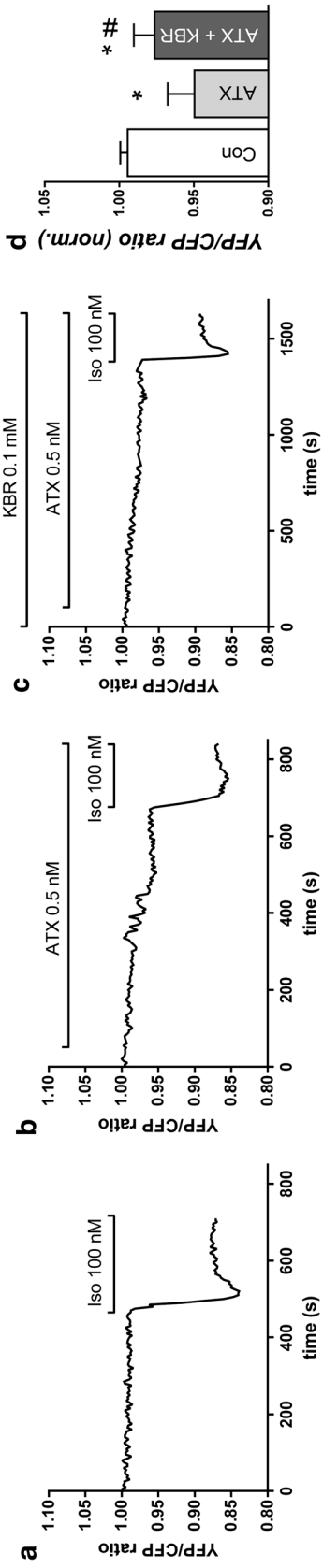

Fig. 3 Effects of late I_{Na} augmentation on intracellular cAMP levels in ventricular cardiomyocytes from EPAC-camps transgenic mice. Representative FRET-recordings during 1 Hz field stimulation showing **a** untreated control, subsequently treated with isoproterenol (100 nmol/L), **b** ATX-II (0.5 nmol/L) and subsequent isoproterenol treatment (100 nmol/L) as well as **c** CMs preincubated with KB-R7943 (0.1 mmol/L) and incubated with ATX-II and subsequently isoproterenol (100 nmol/L). **d** Quantification of response of YFP/CFP ratio; n(mice/cells) = 3/9 vs. 4/13 vs. 4/14. *significant vs. control; #significant vs. ATX ($P < 0.05$)

using okadaic acid, respectively. As shown before, the basal Ca^{2+} spark frequency (CaSpF) was significantly increased by ATX-II (CaSpF ATX-II vs. control = 1.67 ± 0.25 vs. 0.44 ± 0.09 × 100 μm^{-1} s^{-1}, $P < 0.05$, increase by 278 ± 57%, Fig. 4b). Interestingly, additional inhibition of PP2A did not significantly influence ATX-II dependent increase in CaSpF (ATX-II + OA 10 nmol/L vs. ATX-II = 1.69 ± 0.26 vs. 1.67 ± 0.25 × 100 μm^{-1} s^{-1}, $P = 0.97$, Fig. 4b) nor Ca^{2+}-spark amplitude (F/F_0: 1.51 ± 0.012 vs. 1.50 ± 0.01, $P = 0.84$, Fig. 4c), Ca^{2+}-spark width (1.89 ± 0.07 vs. 1.92 ± 0.07 µm, $P = 0.80$, Fig. 4d) and Ca^{2+}-spark duration (22.14 ± 1.040 vs. 20.75 ± 0.88 ms, $P = 0.38$, Fig. 4e). However, an inhibition of both, PP1 and PP2A, resulted in a strong additional increase of CaSpF (ATX-II + OA 100 nM vs. ATX-II = 3.24 ± 0.55 vs. 1.67 ± 0.25 × 100 μm^{-1} s^{-1}, $P < 0.01$, Fig. 4b), Ca^{2+}-spark width (2.35 ± 0.08 vs. 1.92 ± 0.07 ms, $P < 0.001$, Fig. 4d) and Ca^{2+} spark duration (27.53 ± 1.14 vs. 20.75 ± 0.88 ms, $P < 0.001$, Fig. 4e), whereas Ca^{2+} spark amplitude remained unchanged (F/F_0: 1.51 ± 0.01 vs. 1.50 ± 0.01, $P = 0.84$, Fig. 4c).

Effects of late I_{Na} augmentation and PP1 and PP2A inhibition on systolic Ca^{2+} release and SR Ca^{2+} load

Functional influences of additional phosphatase inhibition on Ca^{2+} handling were addressed by epifluorescence microscopy measurements (Fura-2-AM). Cardiomyocytes were stimulated at 1 Hz and systolic Ca^{2+} transients were recorded (Fig. 5a). Additionally, caffeine was applied to quantify SR Ca^{2+} content (Fig. 5a). As shown before, augmentation of late I_{Na} did not significantly affect systolic Ca^{2+} transient amplitude (F_{340}/F_{380}: ATX-II vs. control = 0.31 ± 0.03 vs. 0.21 ± 0.02, $P = 0.09$, Fig. 5b), SR Ca^{2+} reuptake time (RT_{80}: 0.37 ± 0.01 vs. 0.33 ± 0.01, $P = 0.40$, Fig. 5c), as well as the amplitude of caffeine-induced Ca^{2+} transients (F_{340}/F_{380}: 0.46 ± 0.05 vs. 0.48 ± 0.05, $P = 0.87$, Fig. 5d). In line with the confocal data, additional PP2A inhibition did not alter ATX-II induced effects on systolic Ca^{2+} transients, SR Ca^{2+} reuptake time (RT_{80}) or SR Ca^{2+} content (Fig. 5b–d). In contrast, inhibition of both, PP1 and PP2A, yielded a strong additional increase of systolic Ca^{2+} transient amplitude by 66 ± 15% (F_{340}/F_{380}: ATX-II + OA 100 nmol/L vs. ATX-II = 0.52 ± 0.05 vs. 0.31 ± 0.03, $P < 0.001$, Fig. 5b) compared to sole ATX-II treatment, while the decay time of systolic Ca^{2+} transients (RT_{80}: 0.30 ± 0.01 vs.

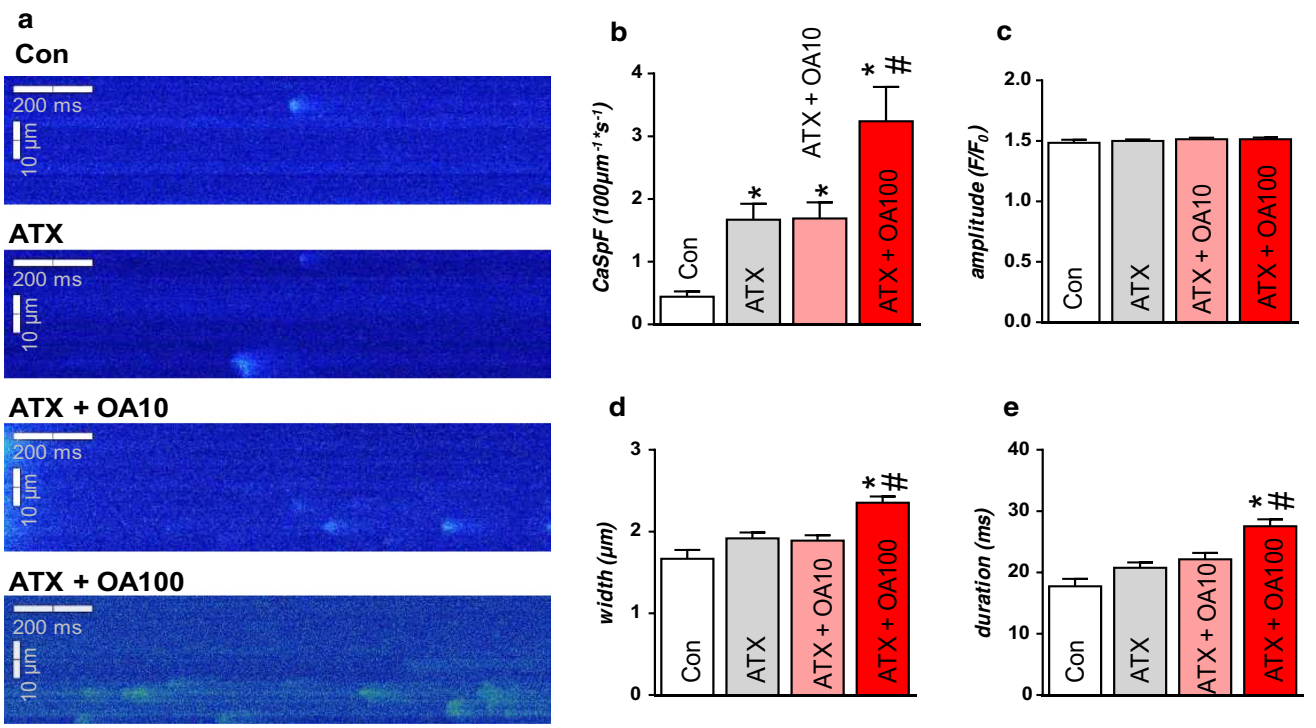

Fig. 4 Effects of PP1/PP2A inhibition on late I_{Na} dependent induction of the SR Ca^{2+} leak. **a** Representative confocal line scans of murine ventricular cardiomyocytes and respective quantification of **b** CaSpF, as well as **c** amplitude, **d** width and **e** duration of detected Ca^{2+} sparks. $N = 10$, n (cells/sparks) = 64/72 vs. 74/188 vs. 76/185 vs. 62/272. *significant vs. control; #significant vs. ATX ($P < 0.05$). Drug concentrations: ATX-II 5 nmol/L; OA10 10 nmol/L; OA100 100 nmol/L

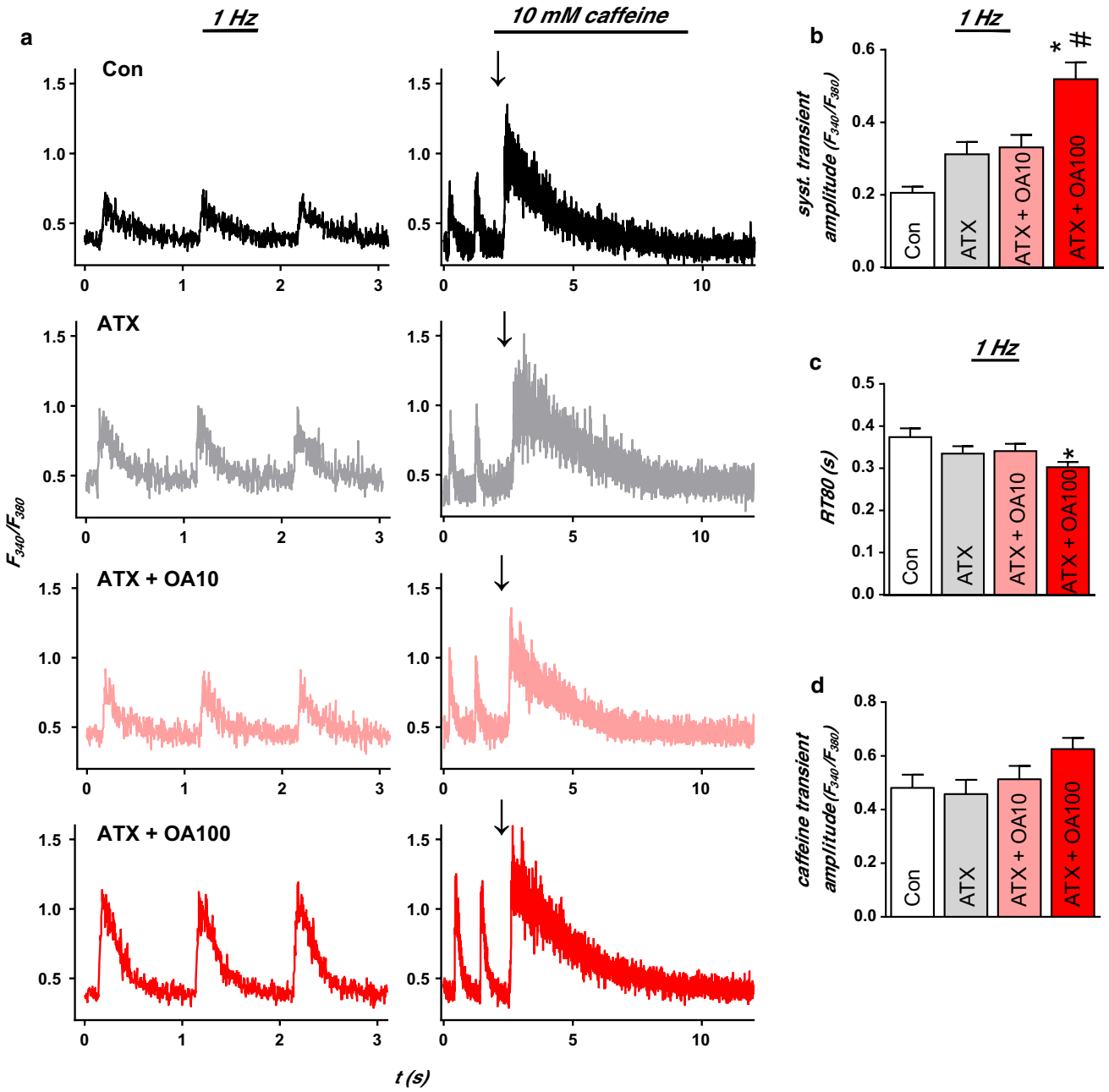

Fig. 5 Effects of late I_{Na} augmentation and PP1/PP2A inhibition on Ca^{2+} cycling properties of murine ventricular cardiomyocytes (epifluorescence microscopy, Fura-2-AM). **a** Representative original recordings of systolic (1 Hz, left) and caffeine-induced Ca^{2+} transients (right, arrow indicates caffeine application) and respective quantification of **b** systolic Ca^{2+} transient amplitude and **c** decay kinetics (RT_{80}) ($N = 7$, n (cells) = 21 vs. 34 vs. 26 vs. 40), as well as **d** amplitude (peak h) of caffeine-induced Ca^{2+} transients ($N = 7$, n (cells) = 14 vs. 7 vs. 10 vs. 13). *significant vs. control; #significant vs. ATX ($P < 0.05$). Drug concentrations: ATX-II 5 nmol/L; OA10 10 nmol/L; OA100 100 nmol/L

0.33 ± 0.02 s, $P = 0.40$, Fig. 5c), as well as the amplitude of caffeine-induced Ca^{2+} transients (F_{340}/F_{380}: 0.63 ± 0.04 vs. 0.46 ± 0.05, $P = 0.13$, Fig. 5d) were not significantly reduced.

Effects of PP1 activation on late I_{Na} dependent induction of the SR Ca^{2+} leak

As PP1 inhibition aggravated late I_{Na} dependent disruption of Ca^{2+} homeostasis we hypothesized that PP1 activation may have beneficial influence on RyR2 stability. To investigate the impact of selective phosphatase 1

activation on diastolic SR Ca^{2+} leak we performed confocal microscopy scans (Fluo-3-AM) using a PP1-specific phosphatase disrupting peptide (PDP3) and its inactive form (PDP3m) in identical concentrations (1 µmol/L). Again, the basal CaSpF was profoundly increased by ATX-II treatment (CaSpF ATX-II vs. control = 1.28 ± 0.22 vs. 0.28 ± 0.06 × 100 μm^{-1} s^{-1}, $P < 0.001$, increase by 355 ± 77%, Fig. 6b). As expected, the inactive peptide PDP3m did not influence late I_{Na} dependent induction of CaSpF as well as Ca^{2+}-spark width and duration (Figs. 6b, d, e) whereas a small reduction of Ca^{2+}-spark amplitude could be observed (F/F0 = 1.56 ± 0.015 vs. 1.62 ± 0.18, $P < 0.05$). Importantly, however, a selective activation of PP1 by PDP3 yielded a strong reduction of CaSpF (CaSpF ATX-II + PDP3 vs. ATX-II = 0.47 ± 0.09 vs. 1.28 ± 0.218 × 100 μm^{-1} s^{-1}, $P < 0.01$, reduction by 63 ± 7%, Fig. 6b). The amplitude of Ca^{2+} sparks (ATX-II + PDP3 vs. ATX-II = 1.58 ± 0.02 vs. 1.62 ± 0.02, $P = 0.35$, Fig. 6c), Ca^{2+} spark width (1.08 ± 0.05 vs. 1.25 ± 0.04 µm, $P = 0.10$, Fig. 6d) and Ca^{2+} spark duration (23.61 ± 1.46 vs. 29.33 ± 1.52 ms, $P = 0.07$, Fig. 6e) were not significantly altered.

Effects of late I_{Na} augmentation and PP1 activation on systolic Ca^{2+} release and SR Ca^{2+} load

To investigate if selective phosphatase 1 activation also impacts systolic Ca^{2+} release and diastolic Ca^{2+} reuptake in the setting of an elevated late I_{Na}, epifluorescence microscopy measurements (Fura-2-AM) were performed as described before (Fig. 7a). In this dataset, augmentation of late I_{Na} led to an increase of systolic Ca^{2+} transient amplitude compared to untreated control (F_{340}/F_{380}: ATX-II vs. control = 0.23 ± 0.02 vs. 0.13 ± 0.01, $P < 0.001$, increases by 79 ± 19%, Fig. 7b) without affecting SR Ca^{2+} reuptake time (RT_{80}: 0.49 ± 0.02 vs. 0.42 ± 0.03 s, $P = 0.16$, Fig. 7c) and the amplitude of caffeine-induced Ca^{2+} transients (F_{340}/F_{380}: 0.35 ± 0.05 vs. 0.33 ± 0.085, $P = 0.97$, Fig. 7d). As expected, adding the inactive control peptide PDP3m did not alter ATX-II induced effects on systolic Ca^{2+}-transients, decay kinetics (RT_{80}) and SR-Ca^{2+}-content (Fig. 7b–d). Interestingly and in contrast to the effect on SR Ca^{2+} leak (see above) a selective activation of PP1 by novel PDP3 did not show any effects on amplitude (F_{340}/F_{380}: ATX-II + PDP3 vs. ATX-II = 0.20 ± 0.03 vs. 0.23 ± 0.02, $P = 0.61$, Fig. 7b) and decay kinetics of systolic Ca^{2+} transients (RT_{80}:

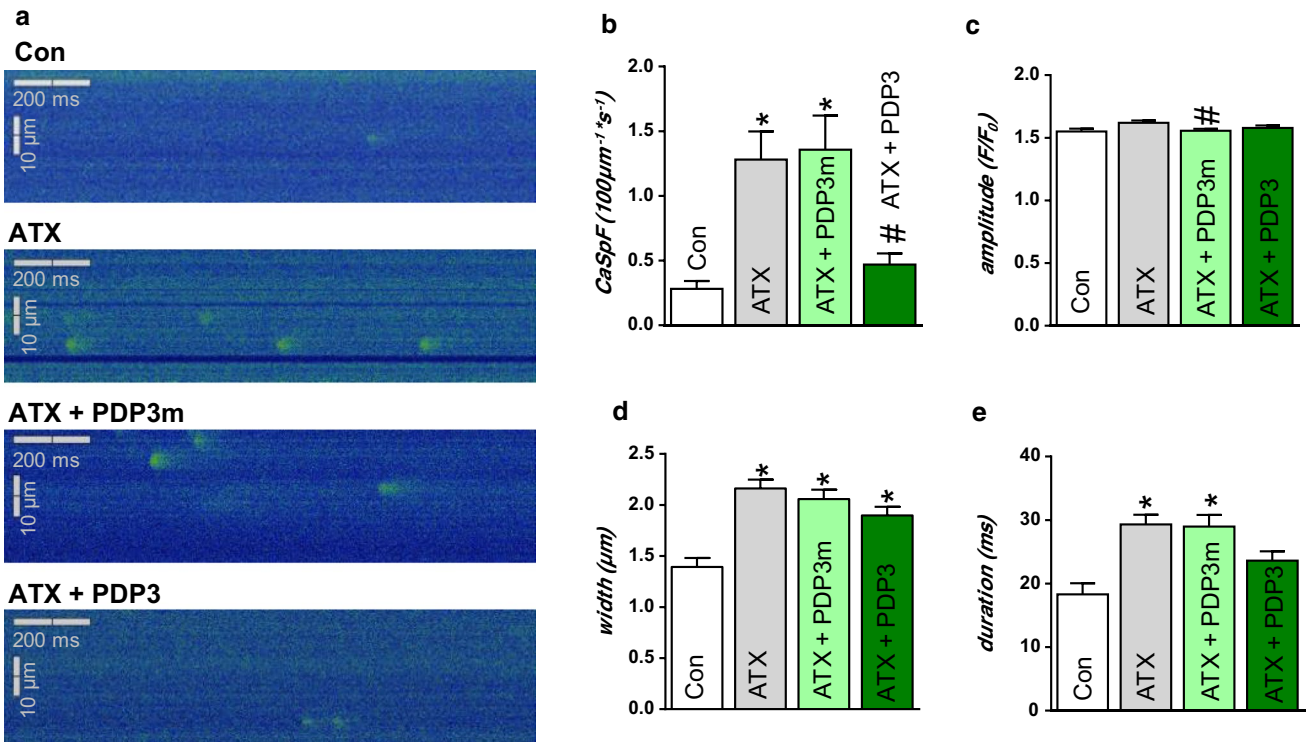

Fig. 6 Effects of PP1 activation on late I_{Na} dependent induction of the SR Ca^{2+} leak. **a** Representative confocal line scans of murine ventricular cardiomyocytes and respective quantification of **b** CaSpF, as well as **c** amplitude, **d** width and **e** duration of detected Ca^{2+} sparks. $N = 4$, n (cells/sparks) = 80/61 vs. 69/186 vs. 63/178 vs. 74/100. *significant vs. control; #significant vs. ATX ($P < 0.05$). Drug concentrations: ATX-II 5 nmol/L; PDP3m 1 µmol/L; PDP3 1 µmol/L

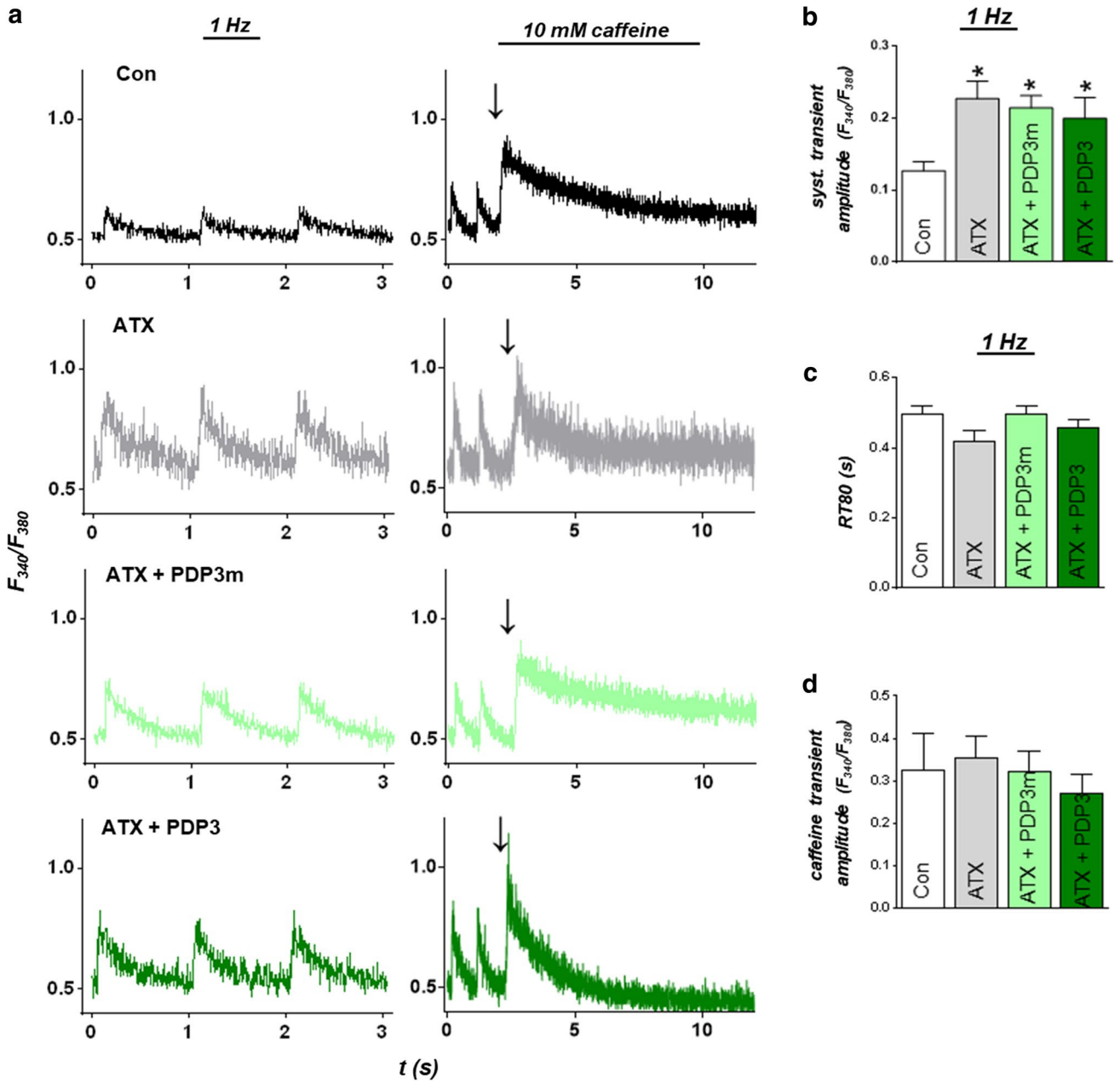

Fig. 7 Effects of late I_{Na} augmentation and PP1 activation on calcium-cycling properties of murine ventricular cardiomyocytes (epifluorescence microscopy, Fura-2-AM). **a** Representative original recordings of systolic (1 Hz, left) and caffeine-induced Ca^{2+}-transients (right, arrow indicates caffeine application) and respective quantification of **b** systolic Ca^{2+}-transient amplitude and **c** decay kinetics (RT_{80}) ($N=6$, n (cells)$=27$ vs. 28 vs. 19 vs. 26), as well as **d** amplitude (peak h) of caffeine-induced Ca^{2+}-transients ($N=6$, n (cells)$=10$ vs. 11 vs. 8 vs. 9). *significant vs. control; #significant vs. ATX ($P<0.05$). Drug concentrations: ATX-II 5 nmol/L; PDP3m 1 µmol/L; PDP3 1 µmol/L

0.46 ± 0.02 vs. 0.42 ± 0.03 s, $P=0.62$, Fig. 7c) nor the amplitude of caffeine-induced Ca^{2+} transients (F_{340}/F_{380}: 0.27 ± 0.05 vs. 0.35 ± 0.05, $P=0.85$, Fig. 7d).

Discussion

This study investigates the functional role of cardiac protein kinases and phosphatases in the late I_{Na}-dependent disruption of Ca^{2+} homeostasis. We demonstrate that activation of late I_{Na} in ventricular murine cardiomyocytes results in an increase of diastolic Ca^{2+} loss from the SR.

Furthermore, this study is the first to show that (1) late I_{Na}-dependant induction of the SR Ca^{2+} leak in ventricular myocytes is mediated by synergistic effects of CaMKII and PKA and only occurs if both kinases are activated. (2) PKA is essential to maintain systolic Ca^{2+} release in the setting of an increased diastolic SR Ca^{2+} leak and (3) seems to be activated by a Ca^{2+}-dependent activation of adenylylcyclases. (4) Sole PP2A inhibition does not influence late I_{Na}-dependent SR Ca^{2+} leak induction and systolic Ca^{2+} release whereas (5) an additional inhibition of PP1 further aggravates the diastolic SR Ca^{2+} leak. In line with this, (6) selective PP1-activation successfully reduces the arrhythmogenic SR Ca^{2+} leak and, importantly, does not compromise systolic Ca^{2+} release.

Elevated late I_{Na} potently induces cellular arrhythmic triggers through activation of CaMKII and PKA

It is well accepted that an elevated late I_{Na} is closely linked to the development of contractile dysfunction and cardiac arrhythmias [4]. In line with this, our data show a profound increase of the diastolic SR Ca^{2+} leak upon induction of late I_{Na} by ATX-II. The method of late I_{Na} induction applying ATX-II has been quantified previously in ventricular [32] and atrial [17] cardiomyocytes performing patch-clamp-measurements and was found to approximate the situation found in cardiac disease [23, 35]. While the crucial role of CaMKII (and counteracting phosphatases) in the genesis of arrhythmogenic RyR2 dysregulation in heart failure has been repeatedly shown [3, 6, 15, 16, 18], these studies could demonstrate that the late I_{Na}-dependent increase of SR Ca^{2+} leak is also mediated by CaMKII in ventricular [32] as well as atrial [17] murine cardiomyocytes. However, the latter study additionally showed that, at least in the atria, PKA also plays an important role as a downstream effector of an increased late I_{Na}. To our knowledge, the current study demonstrates for the first time in ventricular cardiomyocytes that the interaction of both kinases is equally essential for mediating late I_{Na}-dependent changes of Ca^{2+} homeostasis as SR Ca^{2+} leak induction could be effectively prevented by the specific CaMKII-inhibitor AIP as well as by the specific PKA-inhibitor H89.

As the SR Ca^{2+} leak not only depends on the properties of diastolic RyR2-closure but also on SR Ca^{2+} load, we additionally investigated Ca^{2+} cycling properties. Interestingly, our data show that late I_{Na} induction has the potential to increase Ca^{2+}-transient-amplitude in ventricular cardiomyocytes without affecting SR-Ca^{2+}-load suggesting that the elevated diastolic loss of Ca^{2+} (SR Ca^{2+} leak) is counterbalanced by an increased Ca^{2+} reuptake into the SR. As Ca^{2+}-transient-amplitude and SR Ca^{2+} load did not change when CaMKII (AIP) was inhibited, a CaMKII-independent mechanism must exist that is activated by late I_{Na} and facilitates the maintenance of SR Ca^{2+} load in the setting of an increased SR Ca^{2+} leak. Indeed, our current data show that PKA-inhibition (H89) leads to decreased Ca^{2+} transient amplitudes. Thus, PKA seems to enhance SR Ca^{2+} reuptake also in ventricular cardiomyocytes upon late I_{Na} augmentation. This effect may well be explained by SERCA2a-disinhibition through PKA-dependent phospholamban (PLN) phosphorylation. The fact that we could not demonstrate a reduced Ca^{2+} transient decay time under sole ATX-II treatment may be attributed to the significantly higher SR Ca^{2+} leak counteracting an increased SERCA2a-activity. In sum, the current data suggest that CaMKII and PKA exert distinct roles in late I_{Na}-dependent disruption of ventricular Ca^{2+} cycling. Whereas CaMKII may primarily alter RyR2 open probability, PKA may maintain SR Ca^{2+} load through SERCA2a activation, which on the one hand preserves systolic Ca^{2+} release and contractility, but on the other hand enables the arrhythmogenic SR-Ca^{2+}-leak to persist.

Increased late I_{Na} leads to cAMP-dependent activation of PKA

Whereas the mechanism of CaMKII-activation in the setting of an elevated late I_{Na} can comprehensibly be explained by Na^+-dependent intracellular Ca^{2+} overload and consecutive activation of CaMKII via calmodulin, the mechanism of PKA-activation by cytoplasmatic Na^+ influx via late I_{Na} was unclear. Therefore, we sought to elucidate, whether PKA-activation by late I_{Na} via Ca^{2+}-dependent activation of adenylylcyclases, as recently demonstrated by our group in atrial myocardium [17], also occurs in ventricular cardiomyocytes. Indeed, FRET-measurements in Epac-camps transgenic mice revealed a significant decrease of the YFP/CFP-ratio after late I_{Na} induction with ATX-II, indicating an increase of cytoplasmatic cAMP-levels. The change in YFP/CFP-ratio made up for 33% of the maximal response upon β-adrenergic stimulation and can thus sufficiently explain PKA activation. It can be presumed that myocardial adenylylcyclases account for the increased cAMP production upon late I_{Na} augmentation. An additional inhibition of NCX-reverse-mode by KB-R7943 led to a reduction of ATX-II-dependent cAMP-production, signifying a Ca^{2+}-dependent activation of intracellular cAMP-production.

Effects of phosphatase-inhibition on late I_{Na}-dependent Ca^{2+} homeostasis

As the late I_{Na}-induced increase of kinase activity leads to deleterious effects on Ca^{2+} cycling properties, we aimed at investigating whether and how modulations of the conversely acting serine-/threonine-phosphatases PP1 and PP2A impacts these effects. The well-established phosphatase

inhibitor okadaic acid (OA) was used in low concentrations (10 nmol/L) to inhibit PP2A or in higher concentrations (100 nmol/L) to inhibit both, PP1 and PP2A [10, 11, 14]. Interestingly, inhibition of PP2A in the setting of an elevated late I_{Na} did not significantly alter SR Ca^{2+} leak and systolic Ca^{2+} transients. However, inhibition of PP1 and PP2A resulted in a further disruption of diastolic RyR2 closure leading to an even higher diastolic SR Ca^{2+} leak. Thus, inhibition of PP1 and PP2A increases cellular arrhythmogenic triggers and further aggravates late I_{Na}-induced disruption of Ca^{2+} homeostasis. In particular, preserved PP1-activity seems to play an important role in counteracting proarrhythmic kinase-mediated RyR2-hyperphosphorylation in the setting of an enhanced late I_{Na}. On the other hand, inhibition of PP1 and PP2A led to an increase of systolic Ca^{2+} transient amplitude compared to sole ATX-II-treatment suggesting a positive inotropic effect. This can conclusively be explained by an increased PLN phosphorylation resulting in an increased SERCA2a-activity. In line with this, publications investigating an adenovirus-based overexpression of endogenous PP1-inhibitor inhibitor-1 (I1) in experimental porcine heart failure models found preserved cardiac output and reduced scar size after myocardial infarction [19] as well as improvement of left atrial and ventricular function and systolic Ca^{2+} release in non-ischemic heart failure [40]. Surprisingly, proarrhythmic effects were not detected. In contrast, data from a mouse model expressing a constitutively active variant of I1 [27] revealed that I1-transgenic mice display improved contractility but develop a higher propensity towards catecholamine-induced ventricular tachycardia and sudden cardiac death. Furthermore, I1-knock out and consecutively increased PP1-activity was shown to be protective against catecholamine-induced arrhythmias in another mouse model [23].

Reduction of late I_{Na}-induced arrhythmic triggers by selective activation of PP1

Since our experiments showed that inhibition of cardiac phosphatases in the setting of an elevated late I_{Na} further disrupts diastolic RyR2-closing properties, we sought to investigate whether a selective activation of PP1 may have antiarrhythmic effects by counteracting increased kinase activity. For selective activation of PP1, the peptide PDP3 (phosphatase-disrupting-peptide-3) was used [14]. The chemical features of this peptide including cell permeability, stability and PP1-activation had been shown in various cell types [9]. To the best of our knowledge, this is the first study to functionally elucidate the effects of PDP3-dependent PP1-activation in the crosstalk between a pharmacologically elevated late I_{Na} and Ca^{2+} homeostasis. Indeed, we could detect a significant reduction of late I_{Na}-induced SR Ca^{2+} leak (CaSpF) upon PDP3-treatment suggesting an antiarrhythmic effect of selective PP1-activation. However, there was a small reduction of the amplitude of Ca^{2+} sparks upon treatment with PDP3m. This effect can rather be categorized unspecific as Ca^{2+} spark amplitude was not significantly different between PDP3 and PDP3m.

These results showing a reduction of SR-Ca^{2+} leak upon PP1 activation seemingly contradict a study postulating that adding PP1 and PP2A to permeabilized rat cardiomyocytes triggers an increased CaSpF and consecutive reduction of SR Ca^{2+} load [20]. However, significant differences in the design of the experiments have to be considered: While both studies investigated previously healthy wild-type animals, we pharmacologically augmented late I_{Na} in our model and induced significant alterations of cellular electrophysiology and Ca^{2+} cycling similar to conditions found in relevant cardiac pathologies. Moreover, an artificial exposure of permeabilized cardiomyocytes to recombinant PP1 and PP2A may result in a non-physiological subcellular distribution of these enzymes. In contrast, PDP3-dependent PP1-activation is based on a disruption of the interaction between PP1 and regulatory subunits releasing active endogenous PP1 catalytic subunits in close proximity to their original molecular targets.

Of note, PP1-activation by PDP3 did not compromise systolic Ca^{2+} release and SR Ca^{2+} load in our experiments suggesting that PDP3-mediated PP1 activation may predominantly take place at RyR2 over PLN in the setting of an elevated late I_{Na}. This is of great relevance since activation of protein phosphatases at PLN is regarded to further compromise SERCA2a-activity and SR Ca^{2+} loading and therapeutic intentions have rather been striving for inhibition of PP activity in this subcellular compartment, e.g. by overexpressing I1 (see above) [19, 40, 41].

Limitations of the study

1. PP2A inhibition was performed using the phosphatase inhibitor okadaic acid (OA) at a concentration of 10 nmol/L (IC50 = 0.1 nmol/L). Higher concentrations (100 nmol/L) were used to additionally inhibit PP1 (IC50 = 15–20 nmol/L) [11]. At 10 nmol/L, a minor inhibition of PP1 cannot be excluded. This, however, did not translate into obvious effects on Ca^{2+} cycling parameters in contrast to effective inhibition of PP1 using OA at a concentration of 100 nmol/L. A specific inhibition of PP1 by adenoviral transfer of mutated active I1-isoforms would have been superior but was technically not feasible in our laboratory.
2. We used ATX-II to pharmacologically increase late I_{Na} in previously healthy, isolated murine cardiomyocytes. Using a similar experimental approach, we have recently shown that ATX-II treatment yields an increase of late

I_{Na} by ~ 60%, which subsequently triggers SR Ca^{2+} leak and delayed after depolarisations (DADs) [32]. The quantitative effect of ATX-II on late I_{Na}, however, has not been re-quantified in the current study.

3. In our study, the inactive control peptide PDP3m led to small changes of Ca^{2+} spark amplitude compared to sole ATX-II treatment (Fig. 6c). These effects may be attributed to unspecific actions of this small peptide molecule and can similarly be observed upon treatment with PDP3. Treatment with the active peptide PDP3, however, additionally reduced Ca^{2+} spark frequency compared to PDP3m, which thus can be attributed to the PP1 activating properties that distinguish PDP3 from PDP3m.

Conclusions

Our study shows that the delicate balance between kinase and phosphatase activity is disrupted by an ATX-II mediated increase in Na^+ influx via late I_{Na}. CaMKII and PKA are both involved in the disturbances of cellular Ca^{2+} cycling upon cytoplasmatic Na^+ overload. PKA seems to be activated by late I_{Na} through Ca^{2+}-dependent activation of adenylylcyclases. Whereas PP2A-inhibition did not alter Ca^{2+} homeostasis in the setting of an increased late I_{Na}, additional inhibition of PP1 aggravated disruption of Ca^{2+} homeostasis suggesting that PP1 is the major functional counterpart of CaMKII at ventricular RyR2. In line with this, a selective PP1 activation yielded a significant reduction of the arrhythmogenic SR Ca^{2+} leak and, importantly, did not affect systolic Ca^{2+} release.

Outlook

It is well established that a pathologically increased activity of cardiac kinases, especially CaMKII, plays a major and causal role in the development of heart failure. Therapeutic measures attenuating kinase activity, like β-blockers and inhibitors of the renin–angiotensin system, have proven beneficial influences on long term outcome of heart failure patients. Our study suggests that an activation of protein phosphatase activity at RyR2 may be an additional promising antiarrhythmic approach. To be translated into clinical practice, however, major hurdles as to organ-specific application, subcellular specificity and even isoform-specific regulation of PP1 and PP2a in different cardiac pathologies [13, 28] will have to be taken into consideration.

Acknowledgements We gratefully acknowledge the technical assistance of K.-C. Hansing and T. Schulte. THF is funded by the Deutsche Forschungsgemeinschaft (DFG) through the SFB 1002 (A11). SS is supported by the Marga und Walter Boll-Stiftung through a research grant. MK is funded by the European Research Council (ERC) through a starting Grant (# 336567).

Compliance with ethical standards

Conflict of interest The authors declare that they have no conflict of interest.

References

1. Amran MS, Homma N, Hashimoto K (2003) Pharmacology of KB-R7943: a Na^+-Ca^{2+} exchange inhibitor. Cardiovasc Drug Rev 21:255–276
2. Antzelevitch C, Nesterenko V, Shryock JC, Rajamani S, Song Y, Belardinelli L (2014) The role of late I_{Na} in development of cardiac arrhythmias. Handb Exp Pharmacol 221:137–168. https://doi.org/10.1007/978-3-642-41588-3_7
3. Beckendorf J, van den Hoogenhof MMG, Backs J (2018) Physiological and unappreciated roles of CaMKII in the heart. Basic Res Cardiol 113:29. https://doi.org/10.1007/s00395-018-0688-8
4. Belardinelli L, Giles WR, Rajamani S, Karagueuzian HS, Shryock JC (2015) Cardiac late Na(+) current: proarrhythmic effects, roles in long QT syndromes, and pathological relationship to CaMKII and oxidative stress. Heart Rhythm 12:440–448. https://doi.org/10.1016/j.hrthm.2014.11.009
5. Belardinelli L, Shryock JC, Fraser H (2006) Inhibition of the late sodium current as a potential cardioprotective principle: effects of the late sodium current inhibitor ranolazine. Heart 92(Suppl 4):iv6–iv14. https://doi.org/10.1136/hrt.2005.078790
6. Belevych AE, Ho H-T, Bonilla IM, Terentyeva R, Schober KE, Terentyev D, Carnes CA, Györke S (2017) The role of spatial organization of Ca^{2+} release sites in the generation of arrhythmogenic diastolic Ca^{2+} release in myocytes from failing hearts. Basic Res Cardiol 112:44. https://doi.org/10.1007/s00395-017-0633-2
7. Borner S, Schwede F, Schlipp A, Berisha F, Calebiro D, Lohse MJ, Nikolaev VO (2011) FRET measurements of intracellular cAMP concentrations and cAMP analog permeability in intact cells. Nat Protoc 6:427–438. https://doi.org/10.1038/nprot.2010.198
8. Calebiro D, Nikolaev VO, Gagliani MC, de Filippis T, Dees C, Tacchetti C, Persani L, Lohse MJ (2009) Persistent cAMP-signals triggered by internalized G-protein-coupled receptors. PLoS Biol 7:e1000172. https://doi.org/10.1371/journal.pbio.1000172
9. Chatterjee J, Beullens M, Sukackaite R, Qian J, Lesage B, Hart DJ, Bollen M, Kohn M (2012) Development of a peptide that selectively activates protein phosphatase-1 in living cells. Angew Chem Int Ed Engl 51:10054–10059. https://doi.org/10.1002/anie.201204308
10. Chatterjee J, Köhn M (2013) Targeting the untargetable: recent advances in the selective chemical modulation of protein phosphatase-1 activity. Curr Opin Chem Biol 17:361–368. https://doi.org/10.1016/j.cbpa.2013.04.008
11. Cohen P (1989) The structure and regulation of protein phosphatases. Annu Rev Biochem 58:453–508. https://doi.org/10.1146/annurev.bi.58.070189.002321
12. Edelstein A, Amodaj N, Hoover K, Vale R, Stuurman N (2010) Computer control of microscopes using microManager. Curr Protoc Mol Biol Chapter 14(Unit14):20. https://doi.org/10.1002/0471142727.mb1420s92
13. Eleftheriadou O, Boguslavskyi A, Longman MR, Cowan J, Francois A, Heads RJ, Wadzinski BE, Ryan A, Shattock MJ, Snabaitis AK (2017) Expression and regulation of type 2A protein phosphatases

and alpha4 signalling in cardiac health and hypertrophy. Basic Res Cardiol 112:37. https://doi.org/10.1007/s00395-017-0625-2
14. Fahs S, Lujan P, Kohn M (2016) Approaches to study phosphatases. ACS Chem Biol 11:2944–2961. https://doi.org/10.1021/acschembio.6b00570
15. Fischer TH, Eiringhaus J, Dybkova N, Forster A, Herting J, Kleinwachter A, Ljubojevic S, Schmitto JD, Streckfuss-Bomeke K, Renner A, Gummert J, Hasenfuss G, Maier LS, Sossalla S (2014) Ca(2+)/calmodulin-dependent protein kinase II equally induces sarcoplasmic reticulum Ca(2+) leak in human ischaemic and dilated cardiomyopathy. Eur J Heart Fail 16:1292–1300. https://doi.org/10.1002/ejhf.163
16. Fischer TH, Eiringhaus J, Dybkova N, Saadatmand A, Pabel S, Weber S, Wang Y, Kohn M, Tirilomis T, Ljubojevic S, Renner A, Gummert J, Maier LS, Hasenfuss G, El-Armouche A, Sossalla S (2018) Activation of protein phosphatase 1 by a selective phosphatase disrupting peptide reduces sarcoplasmic reticulum Ca(2+) leak in human heart failure. J Heart Fail, Eur. https://doi.org/10.1002/ejhf.1297
17. Fischer TH, Herting J, Mason FE, Hartmann N, Watanabe S, Nikolaev VO, Sprenger JU, Fan P, Yao L, Popov AF, Danner BC, Schondube F, Belardinelli L, Hasenfuss G, Maier LS, Sossalla S (2015) Late INa increases diastolic SR-Ca^{2+}-leak in atrial myocardium by activating PKA and CaMKII. Cardiovasc Res 107:184–196. https://doi.org/10.1093/cvr/cvv153
18. Fischer TH, Herting J, Tirilomis T, Renner A, Neef S, Toischer K, Ellenberger D, Forster A, Schmitto JD, Gummert J, Schondube FA, Hasenfuss G, Maier LS, Sossalla S (2013) Ca^{2+}/calmodulin-dependent protein kinase II and protein kinase A differentially regulate sarcoplasmic reticulum Ca^{2+} leak in human cardiac pathology. Circulation 128:970–981. https://doi.org/10.1161/CIRCULATIONAHA.113.001746
19. Fish KM, Ladage D, Kawase Y, Karakikes I, Jeong D, Ly H, Ishikawa K, Hadri L, Tilemann L, Muller-Ehmsen J, Samulski RJ, Kranias EG, Hajjar RJ (2013) AAV9.I-1c delivered via direct coronary infusion in a porcine model of heart failure improves contractility and mitigates adverse remodeling. Circ Heart Fail 6:310–317. https://doi.org/10.1161/circheartfailure.112.971325
20. Hell JW (2014) CaMKII: claiming center stage in postsynaptic function and organization. Neuron 81:249–265. https://doi.org/10.1016/j.neuron.2013.12.024
21. Isenberg G, Ravens U (1984) The effects of the Anemonia sulcata toxin (ATX II) on membrane currents of isolated mammalian myocytes. J Physiol 357:127–149. https://doi.org/10.1113/jphysiol.1984.sp015493
22. Ju YK, Saint DA, Gage PW (1996) Hypoxia increases persistent sodium current in rat ventricular myocytes. J Physiol 497(Pt 2):337–347. https://doi.org/10.1113/jphysiol.1996.sp021772
23. Landstrom AP, Dobrev D, Wehrens XHT (2017) Calcium signaling and cardiac arrhythmias. Circ Res 120:1969–1993. https://doi.org/10.1161/CIRCRESAHA.117.310083
24. Maier LS, Sossalla S (2013) The late Na current as a therapeutic target: where are we? J Mol Cell Cardiol 61:44–50. https://doi.org/10.1016/j.yjmcc.2013.03.001
25. Maltsev VA, Sabbah HN, Higgins RS, Silverman N, Lesch M, Undrovinas AI (1998) Novel, ultraslow inactivating sodium current in human ventricular cardiomyocytes. Circulation 98:2545–2552. https://doi.org/10.1161/01.CIR.98.23.2545
26. Maltsev VA, Undrovinas A (2008) Late sodium current in failing heart: friend or foe? Prog Biophys Mol Biol 96:421–451. https://doi.org/10.1016/j.pbiomolbio.2007.07.010
27. Marks AR (2013) Calcium cycling proteins and heart failure: mechanisms and therapeutics. J Clin Invest 123:46–52. https://doi.org/10.1172/JCI62834
28. Meyer-Roxlau S, Lämmle S, Opitz A, Künzel S, Joos JP, Neef S, Sekeres K, Sossalla S, Schöndube F, Alexiou K, Maier LS, Dobrev D, Guan K, Weber S, El-Armouche A (2017) Differential regulation of protein phosphatase 1 (PP1) isoforms in human heart failure and atrial fibrillation. Basic Res Cardiol 112:43. https://doi.org/10.1007/s00395-017-0635-0
29. Picht E, Zima AV, Blatter LA, Bers DM (2007) SparkMaster: automated calcium spark analysis with ImageJ. Am J Physiol Cell Physiol 293:C1073–C1081. https://doi.org/10.1152/ajpcell.00586.2006
30. Rivolta I, Abriel H, Tateyama M, Liu H, Memmi M, Vardas P, Napolitano C, Priori SG, Kass RS (2001) Inherited Brugada and long QT-3 syndrome mutations of a single residue of the cardiac sodium channel confer distinct channel and clinical phenotypes. J Biol Chem 276:30623–30630. https://doi.org/10.1074/jbc.M104471200
31. Ronchi C, Torre E, Rizzetto R, Bernardi J, Rocchetti M, Zaza A (2017) Late sodium current and intracellular ionic homeostasis in acute ischemia. Basic Res Cardiol 112:12. https://doi.org/10.1007/s00395-017-0602-9
32. Sag CM, Mallwitz A, Wagner S, Hartmann N, Schotola H, Fischer TH, Ungeheuer N, Herting J, Shah AM, Maier LS, Sossalla S, Unsold B (2014) Enhanced late I_{Na} induces proarrhythmogenic SR Ca leak in a CaMKII-dependent manner. J Mol Cell Cardiol 76:94–105. https://doi.org/10.1016/j.yjmcc.2014.08.016
33. Shryock JC, Song Y, Rajamani S, Antzelevitch C, Belardinelli L (2013) The arrhythmogenic consequences of increasing late I_{Na} in the cardiomyocyte. Cardiovasc Res 99:600–611. https://doi.org/10.1093/cvr/cvt145
34. Sossalla S, Kallmeyer B, Wagner S, Mazur M, Maurer U, Toischer K, Schmitto JD, Seipelt R, Schondube FA, Hasenfuss G, Belardinelli L, Maier LS (2010) Altered Na(+) currents in atrial fibrillation effects of ranolazine on arrhythmias and contractility in human atrial myocardium. J Am Coll Cardiol 55:2330–2342. https://doi.org/10.1016/j.jacc.2009.12.055
35. Sossalla S, Wagner S, Rasenack EC, Ruff H, Weber SL, Schondube FA, Tirilomis T, Tenderich G, Hasenfuss G, Belardinelli L, Maier LS (2008) Ranolazine improves diastolic dysfunction in isolated myocardium from failing human hearts—role of late sodium current and intracellular ion accumulation. J Mol Cell Cardiol 45:32–43. https://doi.org/10.1016/j.yjmcc.2008.03.006
36. Sprenger JU, Perera RK, Gotz KR, Nikolaev VO (2012) FRET microscopy for real-time monitoring of signaling events in live cells using unimolecular biosensors. J Vis Exp 25:e4081. https://doi.org/10.3791/4081
37. Toischer K, Hartmann N, Wagner S, Fischer TH, Herting J, Danner BC, Sag CM, Hund TJ, Mohler PJ, Belardinelli L, Hasenfuss G, Maier LS, Sossalla S (2013) Role of late sodium current as a potential arrhythmogenic mechanism in the progression of pressure-induced heart disease. J Mol Cell Cardiol 61:111–122. https://doi.org/10.1016/j.yjmcc.2013.03.021
38. Ward CA, Bazzazi H, Clark RB, Nygren A, Giles WR (2006) Actions of emigrated neutrophils on Na(+) and K(+) currents in rat ventricular myocytes. Prog Biophys Mol Biol 90:249–269. https://doi.org/10.1016/j.pbiomolbio.2005.07.003
39. Ward CA, Giles WR (1997) Ionic mechanism of the effects of hydrogen peroxide in rat ventricular myocytes. J Physiol 500(Pt 3):631–642
40. Watanabe S, Ishikawa K, Fish K, Oh JG, Motloch LJ, Kohlbrenner E, Lee P, Xie C, Lee A, Liang L, Kho C, Leonardson L, McIntyre M, Wilson S, Samulski RJ, Kranias EG, Weber T, Akar FG, Hajjar RJ (2017) Protein phosphatase inhibitor-1 gene therapy in a swine model of nonischemic heart failure. J Am Coll Cardiol 70:1744–1756. https://doi.org/10.1016/j.jacc.2017.08.013
41. World Medical Association (2013) World Medical Association Declaration of Helsinki: ethical principles for medical research involving human subjects. JAMA 310:2191–2194. https://doi.org/10.1001/jama.2013.281053